

# NOVEL SEGMENTATION BASED CERVICAL CANCER DETECTION USING DEEP CONVOLUTIONAL BASED NEURAL NETWORK WITH RELU

SOUMYA HARIDAS<sup>1\*</sup>, DR. T. JAYAMALAR<sup>2</sup>

<sup>1\*</sup>Research Scholar, Department of Computer Science, Avinashilingam Institute for Home Science and Higher Education for Women, Coimbatore, Tamil Nadu, India

<sup>2</sup>Assistant Professor, Department of Information Technology, Avinashilingam Institute for Home Science and Higher Education for Women, Coimbatore, Tamil Nadu, India

<sup>1\*</sup>Corresponding Author Email: soumya.smya@gmail.com

<sup>2</sup> Email: jayamalar\_it@avinuty.ac.in

## ABSTRACT

Malignant growth in the cervical area is the fourth most common cause of death in women worldwide. The global burden of cervical cancer has decreased as a result of early screening, which made the disease a preventable one. Early detection and treatment of this cancer may reduce its adverse effects. In this paper, a proposed Deep Convolution-based neural network is used to find cervical cancer. The cervical image is preprocessed utilizing the Anisotropic Diffusion Filter (ADF), in which the edges of the image get preserved. Dragonfly optimization (DA) is used to optimize the weights of ADF. The weighted Fuzzy C-Means (WFCM) clustering method is utilized for segmentation, and makes the weight as optimized in WFCM by using the Grasshopper Optimization Algorithm (GOA). Consequently, a Deep Convolutional Neural Network (Deep CNN) employing a Rectified Linear Unit (ReLU) as the activation function is utilized for the extraction and classification of features. The Deep CNN surpasses alternative classifiers, achieving an accuracy of 97.8% in identifying cervical cancer, as evidenced by the study's findings on the performance of the proposed method relative to existing classifiers.

**Keywords:** *Cervical Cancer, Anisotropic Diffusion Filter (ADF), Dragonfly optimization (DA), weighted Fuzzy C-Means (WFCM), Grasshopper Optimization Algorithm (GOA), Deep Convolutional Neural Network (Deep CNN), Rectified Linear Unit (Relu).*

## 1. INTRODUCTION

The uterine cervix, a vital region of a woman's reproductive system, is susceptible to irregular cell proliferation leading to cervical cancer. Second only to breast cancer, cervical cancer stands as a prevalent threat to women's health. Early detection of cervical cell abnormalities carries significant clinical implications, particularly in the context of early-stage cervical cancer screening. Various screening techniques, such as Pap smear, colposcopy, and HPV testing, play pivotal roles in identifying and diagnosing cervical cancer. Among these methods, Pap smear cell classification holds promise for precise and automated early diagnosis. Accurate classification of Pap smear cell images not only

aids in early identification but also streamlines the diagnostic process for cervical cancer. It is impossible to understate the importance of accurate Pap smear image screening in assisting to identify and diagnose cervical cancer early on. While traditional screening methods like visual examination of the cervix (VIA), cytology through the Pap smear test, colposcopy, biopsy, and HPV-DNA detection involve skilled medical professionals, the subjective nature of cancer diagnosis emphasizes the importance of a pathologist's expertise and experience.

The integration of automated and intelligent screening technologies becomes important in this case. Such technologies can provide valuable support by enhancing the accuracy and efficiency of the screening process,

reducing subjective assessments, and potentially improving early diagnosis outcomes. In the coming sections of this article, we look into the advancements and applications of automated cervical cancer classification techniques, particularly focusing on the utilization of intelligent technologies to augment the traditional screening methods. These advancements aim to contribute to the development of more effective and accessible approaches for early detection and diagnosis of cervical cancer.

## 2. LITERATURE SURVEY

With the advent of computer-based solution for early prediction of cervical cancer, numerous methods were proposed. The freshly released researches indicate that they can be used to determine the stages of various cancer kinds. The conventional approach for early detection of cervical cancer involves a cytology-based screening procedure [1]. However, a significant drawback of this method is its time-consuming nature and the need for specialized knowledge [2]. Hence, it increases the demand for computer-based algorithms to serve the general community.

Lu et al. [3] compared various methods for enhancing the image quality. Methods from the domains such as spatial, frequency, and fuzzy were used during this study. Histogram-based methods along with fuzzy logic-based methods have been proven to be successful. According to the study the author suggests ant colony optimization to automate the assessment of the enhancement factor based on fuzzy-logic, giving a more precise description of the image.

As stated by Deepa and Rao [4], the quasi distribution of photons causes the Poisson noise to be injected into cell pictures. The study's conclusions indicate that an adaptable Wiener filter may be able to successfully reduce Poisson noise. An adaptable Wiener filter can be used to denoise photos even if the image quality varies from one area to another.

By using a technique called bi-histogram equalization, Tang and Isa [5] were able to improve the calibre of grayscale images. A total of two sub-histograms are generated from the input histogram. Clipping the histogram was used to reduce the picture's oversaturation, and

the output that was produced was then equalised and combined to create the final product. A comparison with existing histogram-based enhancement algorithms demonstrates that, on average, the efficiency of the authors' technique is better.

Sharma and Mangat [6], improved the research, by improving the "fuzzy c-means (FCM)" clustering technique. They handled many clusters instead of just one, to strengthen the data clustering. The author proposed integrating segmentation techniques to improve the segmentation accuracy with methods for identifying areas of interest. The Herlev dataset's current accuracy might be enhanced through different feature modifications, enhanced noise reduction, and segmentation (93.7 percent).

In order to improve the boundary of the nucleus, Saha et al. [7] developed a function with a circular shape that restricted the cluster's shape. This was done to give the nucleus a fuller appearance. Extreme learning machine with crow search optimization [ELMCSO] classification was the method for cervical cancer diagnosis proposed by Geetha and Suganya [8]. This study's major goal is to prevent failures by detecting the cervical cell using computerized techniques. Here, the Pap smear image is enhanced using Kaun Filter. The Bayesian Optimization Algorithm is an optimization method used to determine the weight in the kaun filter. It is typically an enhanced KF as a result. Active Contour model was used to segment the rebuilt image. This uses the Analytic Hierarchy Process optimization technique to address the weight upgrade issue. Later, from the segmented region, the solid characteristics are removed which is most important for diagnosing the malignancy.

Devi et al. [9] tested different neural network designs for the goal of diagnosing diseases. In terms of accelerating the detection process, ANN designs like the multilayered perception may indeed be useful. A knowledge-based network and a feed forward network were used here. It helps in mapping the input images with the rules and also to extract the classification features. The network's classification results were excellent, and its accuracy rate was respectable. Using the artificial neural network (ANN) for classification yields more accurate and improved results.

By examining pictures from Pap smears, Athinarayanan et al. [10] created cervical disease classification system. We used the concatenated feature extraction method (CFE), the ERSTCM and CABS descriptors, and the rough set text on co-occurrence matrix to improve it. The effectiveness of the retrieved characteristics can be evaluated using a classifier by correlating them to statistical standards like sensitivity, accuracy and specificity by using classification algorithm (FL-HKSVM). The CFE method outperformed the other two classifiers in terms of performance. By preserving the qualities of the original dataset, feature extraction converts raw information into quantitative attributes that can be managed. Comparatively, it yields superior outcomes when contrasted with applying machine learning directly to raw data. CNNs are frequently used in healthcare applications. It has the capability to autonomously extract features from both time series data and images represented in the frequency domain. These features are then used by a classifier network to perform classification and regression. Deep learning networks are characterized by a substantial number of hidden layers within the neural network. This type of network may accurately predict outcomes by capturing the nonlinear relationship between complex patterns. Deep neural network structures like convolution neural network (CNN) are frequently implemented for image recognition and analysis [11]. To be able to learn any imaginable attribute, a machine will inevitably learn features at numerous levels of abstraction. To enable the system to learn everything, this is required.

The effectiveness of classical machine learning techniques depends heavily on how precisely cells are segmented. Taha et al. [12] suggested a method for classifying cells without segmentation. They used a deep feature learning CNN as part of their strategy. With a rate of 98 percent accuracy, they were able to successfully categorize the Herlev dataset.

Hyeon et al. [13] formulated a prototype proficient in distinguishing healthy and unhealthy cervical cells. The model utilizes a convolutional neural network (CNN) to generate feature vectors from images depicting cervical cells. An SVM classifier was used to train on these collected characteristics, and the overall success rate was 78%. In this paper, a

classification model for prostate cancer is proposed. The model uses deep learning techniques, achieving accuracy rates of 78.1% and 80.1% on testing sets and training sets, respectively.

Manik Sharma et al. provide a robust analysis of diabetes and cancer detection using five distinct insect-based methodologies in their work [14]. Ant Colony Optimization (ACO), Glow Worm Swarm Optimization (GSO), Firefly Algorithm (FA), Artificial Bee Colony (ABC) and Ant Lion Optimization are these five insect-based approaches (ALO). Their research shows that a neural network using an ACO optimization strategy can produce predictions with a higher degree of accuracy.

### 3. PROPOSED METHODOLOGY

The proposed approach to cervical cancer screening is a computer-aided automatic detection system. The general strategy for the discovery component is outlined in Figure 1. The initial cervical image is preprocessed using the Anisotropic Diffusion Filter. Dragonfly optimization can be utilized to improve the ADF's weight in order to reduce the noise and also preserve the edges. The preprocessed image is then used to segment the affected cell by using the Weighted FCM with Grasshopper Enhancement Algorithm (GOA) for productively distinguishing the features such as shape, GLCM highlights and other geometrical features. Comparing the pap smear image with the trained features, these features are used to train the Deep CNN with Relu as an activation function to classify it as benign or malignant. Accuracy, Recall, and Specificity are the performance measurement parameters used to evaluate performance of the cervical image classification.

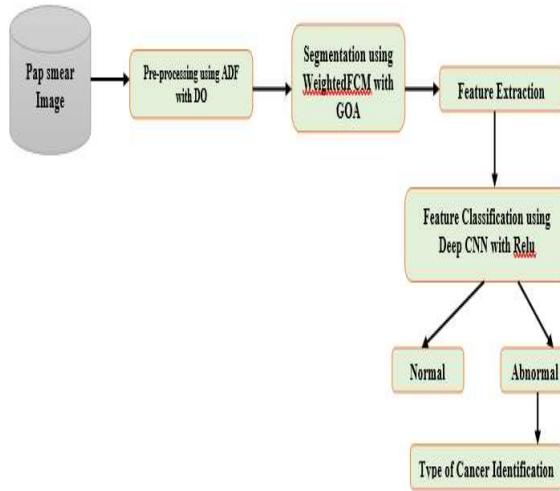


Figure 1: System Architecture of Cervical Cancer Detection

### 3.1. Preprocessing

In many image applications, pre-processing is an essential step because it reduces the input image distortions and eliminates the noise and also improves the quality of an image. Preprocessing functions are typically categorized as radiometric or geometric corrections and are typically performed prior to the primary data analysis and information extraction [18]. Image resizing, Noise Removal, Image Quality, and RGB to gray scale conversion techniques have been used in this paper.

In this proposed work, the process of Preprocessing is as:

1. The pap-smear colour image is converted to a grayscale image.
2. To preserving the edges and reducing the noise in an image by applying the Anisotropic Diffusion Filter.
3. The best weights for the ADF filter were found using Dragonfly Optimization, which effectively preprocess the image. The preprocessing process are shown in figure 2.

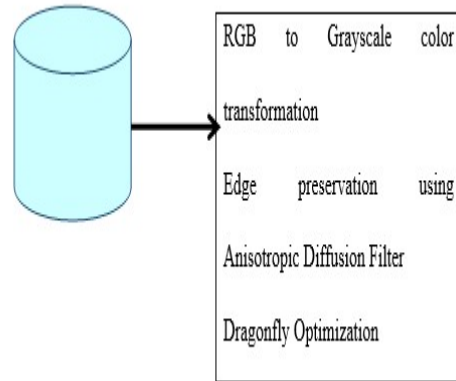


Figure 2: Pre-process

#### 3.1.1 Anisotropic Diffusion Filter

Anisotropic diffusion is a technique that constructs a scale-space by introducing an image into a set of progressively blurred images with varying parameters, employing a diffusion process. In fact, the generalized diffusion equation is approximated and is used to implement anisotropic diffusion, and the equation is applied on the previous image to determine each new image in the group. As a result, the anisotropic diffusion process proceeds iteratively until a sufficient level of smoothing is achieved [15, 16]. The original image is qualitatively smoothed while brightness discontinuities are preserved by anisotropic diffusion [17].

The equation has the potential to modify the diffusion coefficient based on the properties of the image, and it maintains the edge details of the image during denoising.

The diffusion model is expressed as

$$\frac{\partial P}{\partial t} = \text{div}(c(x, y, t)\nabla P) = \nabla c \cdot \nabla P + c(x, y, t)\Delta P \quad (1)$$

Where,

$\Delta$  - Laplacian,  $\nabla$  - the gradient,  $\text{div}(\dots)$  - the divergence operator and  $c(x, y, t)\Delta$  - the diffusion coefficient.

For  $t > 0$  the output is given as  $P(\cdot, t)$ , with larger  $t$  produce images with blur effect.

$c(x, y, t)$  regulates the diffusion rate. It is considered as an image gradient function to preserve edges.

$$c(\|\nabla P\|) = e^{-\left(\frac{\|\nabla P\|}{K}\right)^2} \quad (2)$$

Based on the discrete sampled image, the equation made by Perona and Malik [19] [20] as follows:

$$P_{t+1}^s = IP_t^s + \frac{\lambda}{|\eta^s|} \sum_{p \in \eta} g(|\nabla P_{s,p}(t)|) \nabla P_{s,p}(t) \quad (3)$$

Where, t represents the discrete time,  $I_t^s$  is the discrete image sample.  $\eta^s$  is neighbourhood pixel s,  $|\eta^s|$  gives the count of neighbouring pixels. The image gradient magnitude for the given direction is described by the given formula as:

$$\nabla I_{s,p}(t) = I_t^p - I_t^s, p \in \eta^s \quad (4)$$

### 3.1.2 Dragonfly Optimization:

The natural behaviour of dragonflies served as inspiration for the development of the Dragonfly Algorithm (DA). The natural swarming patterns of dragonflies, as both static and dynamic, served as the basis for this algorithm. The static along with dynamic swarming are two imperative periods of advancement: (1) Exploration is employed to identify promising regions within the search space and (2) Exploitation that contributes to the convergence of the global optimum. Flowchart for Dragonfly Algorithm is shown in Figure 3.

The cycle begins with an introduction stage, followed by N emphases to recognize the neighbouring pixels of an image and it performs the exploration and the exploitation repeatedly. A decision process is carried out at the end to identify the optimal image edges.

During the exploration and exploitation, the dragonflies are guided by five factors: specifically, the food factor, the enemy factor, separation, alignment, and cohesion. The factors are regulated by the following components: (i) separation weight denoted as "s," (ii) alignment weight represented by "a," (iii) cohesion weight indicated as "c," (iv) food factor labeled as "f," (v) enemy factor denoted by "e," and (vi) inertia weight identified as "w". To ensure the swarm's survival, the objective is to attract it towards food sources and divert it away from potential threats. In each iteration, the weakest solution is identified as the enemy, while the best solution serves as the food source. During the exploration phase, weight adjustments promote strong alignment and discourage cohesion. In the exploitation phase, there is an emphasis on high alignment but low cohesion. To enable the

algorithm to move from exploration to exploitation phase, the weights are altered.

The collision of one dragonfly with the other in the neighbouring pixels is avoided by calculating the separation factor as

$$Sf^i = -\sum_{j=1}^N X^j - X^i \quad (5)$$

Where  $X^i$  - the current position,  $X^j$  - the position of neighbour, N - number of adjacent dragonflies.

To match the speed of one dragonfly to another the alignment weight  $Aw^i$  is computed as

$$Aw^i = \frac{\sum_{j=1}^N V^j}{N} \quad (6)$$

Where  $V^j$  is the speed of the  $j^{\text{th}}$  neighbour of dragonfly.

The Cohesion factor is calculated based on the affinity of a single dragonfly towards the neighbourhood's mass centre as:

$$Cf^i = \frac{\sum_{j=1}^N X^j}{N} - X^i \quad (7)$$

The Food factor is calculated based on the dragonfly's affinity towards the food source

$$Ff^i = X_f - X^i \quad (8)$$

Where  $X_f$  represents the food source location.

The computation of the Enemy factor is determined by the deviation of a dragonfly from a designated enemy

$$Ef^i = X_e + X^i \quad (9)$$

Where,  $X_e$  is the enemy position.

The step vector  $\Delta X_{t+1}^i$  can be calculated to imitate the movements thus updating the location of the dragonflies within the search space.

$$\Delta X_{t+1}^i = (swSf^i + awAw^i + cwCf^i + fwFf^i + ewEf^i) + \omega \Delta X_t^i \quad (10)$$

Here, the symbols represent specific weights and parameters: sw for separation weight, aw for alignment weight, cw for cohesion weight, fw for the weight of the food factor, ew for the weight of the enemy factor,  $\omega$  for inertia weight, and t for the counter. The dragonflies' positions can be updated following the calculation of the step vector  $\Delta X_{t+1}^i$  using

$$X_{t+1}^i = X_t^i + \Delta X_{t+1}^i \quad (11)$$

All of the dragonflies will unite into a single dynamic swarm during the final optimization stage, moving toward the global optimal solution. When no other artificial dragonflies left in the search space, they use the Lévy flight mechanism [21] to move around. Dragonflies

without neighbors are given a random position by performing a random walk. The position can be updated using the

$$X_{t+1}^i = X_t^i + Levy(d) \times X_t^i \quad (12)$$

Here, the symbol t signifies the current iteration count, while d is used to denote the dimensionality of the position vectors. At last the optimum pixel intensity value can be found to identify the optimized edges of an image from the enhanced image using anisotropic diffusion Filter.

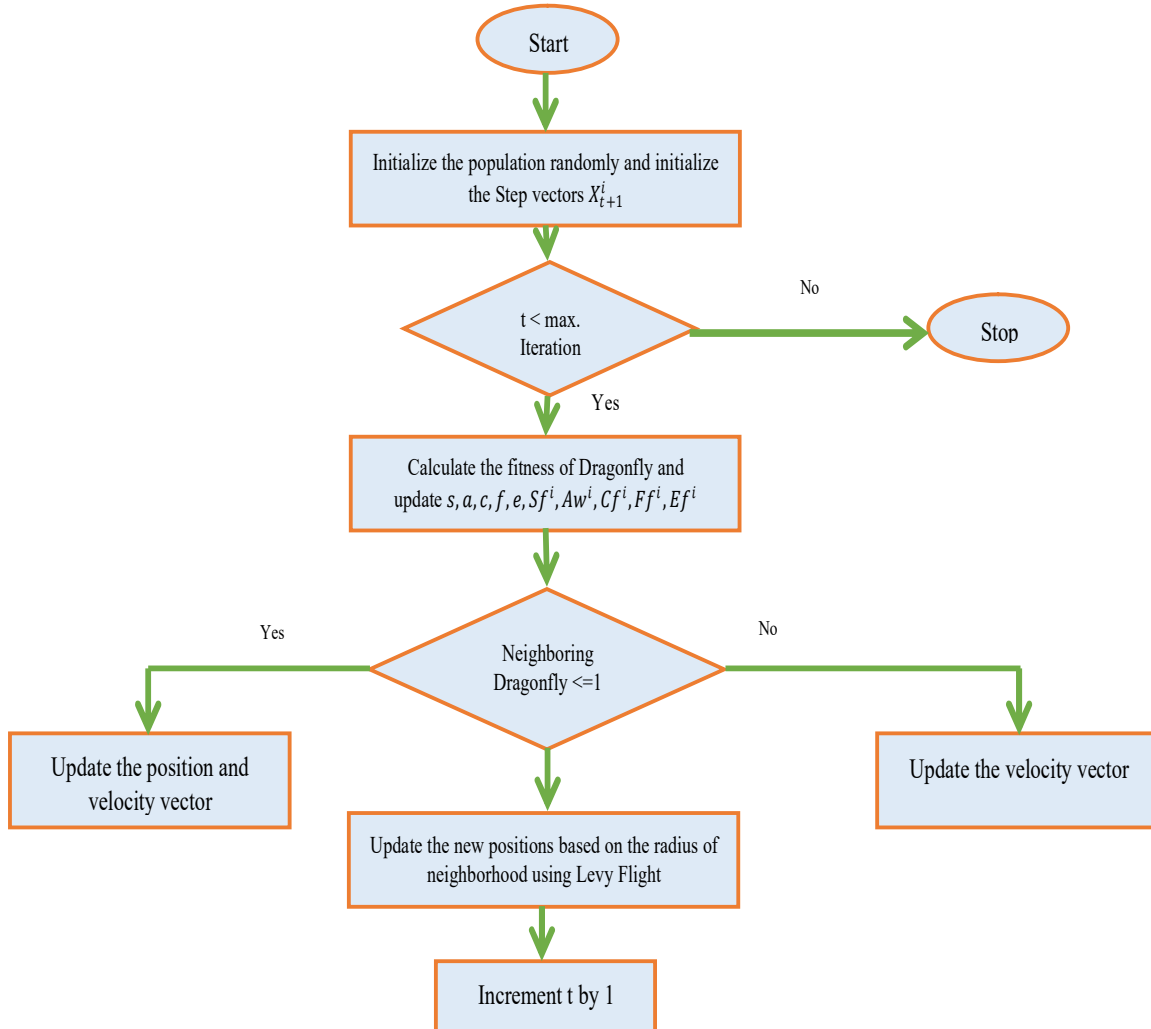


Figure 3: Flowchart for Dragonfly Algorithm

### 3.2 Segmentation Weighted FCM

In computer vision, image segmentation can be used in a variety of real-world System. Medical imaging, image retrieval with content, video surveillance, object detection and recognition, and Automatic Traffic Control systems are all important applications of image segmentation. In order to facilitate with diagnosis and treatment planning, segmentation algorithms have lately been applied in the medical industry

to extract relevant information from medical images.

Segmentation is the process of splitting an image into different parts by grouping together pixels of the same type based on factors such as color, intensity, texture, or volume. During the past ten years, numerous approaches to segmentation have been proposed in an effort to raise the precision level and to improve the efficiency of the results. Image segmentation techniques for medical images are widely used to

separate input images and to get important information about the area of interest. The ROI can be lesions, cancerous cells, or tumour tissues. The effects of division are exceptionally vital and significant and requests high accuracy level for all intents and purposes based on these outcomes that the specialist recommends finding to their patients.

**3.3 Weighted Fuzzy C-Means (WFCM) algorithm with Grasshopper Optimization Algorithm:**

In the weighted FCM, the weighting factor has been utilized to improve the cluster center for the FCM. This was proposed in the previous work. In order to improve the weight in WFCM and made as an optimal weight has been proposed through the Grasshopper Optimization Algorithm (GOA).

The proposed IWFCM technique involves mapping input data into a higher-dimensional feature space through a nonlinear transformation. Subsequently, Fuzzy C-Means (FCM) is applied within this feature space. The Kernel Weighted Fuzzy C-Means method is employed to minimize the resulting objective function, as discussed in reference [23].

$$Y\omega = \sum_{i=1}^k \sum_{j=1}^n b_{ij}^l \|\omega(x_j) - \omega(v_i)\|^2 \quad (13)$$

Where  $\omega(v_i)$  is the feature space centre of cluster  $i$ ,  $b_{ij}$  indicates if  $x_j$  is a member of cluster  $i$ , and  $\omega$  is used to map input space  $X$  to feature space  $F$ .

**3.3.1 Grasshopper Optimization Algorithm**

The natural swarming behavior of grasshoppers serves as inspiration for the grasshopper optimization algorithm. Saremi et al. first proposed to decide the ideal state of systematic structures [22]. The grasshopper's individual movement is influenced by three main factors: social relationship, force of gravity, and wind advection [24, 25]. Below is a mathematical depiction of their swarm activity.:

$$X^i = r_1 S^i + r_2 G^i + r_3 A^i \quad (14)$$

where  $r_1, r_2$  and  $r_3$  are the random numbers,  $S^i, G^i, A^i$  are social relationship, gravity force and wind advection respectively. To improve the version of equation (14), in order to solve the best optimization problems using the equation (15)

$$X_d^i = c \left( \sum_{j=1, j \neq i}^n c \frac{UB_d - LB_d}{2} S(|x_d^j - x_d^i|) \frac{x_d^j - x_d^i}{d^{ij}} \right) + \text{best}, \quad (15)$$

The upper bound ( $UB_d$ ) and lower bound ( $LB_d$ ) represent the limits in the  $d^{\text{th}}$  dimension, while "best" denotes the current optimal value in that specific dimension within the solution space  $d^{ij} = |x^j - x^i|$  shows the distance between the  $i^{\text{th}}$  and  $j^{\text{th}}$  grasshoppers ( $r$ ) is calculated using  $s(r) = fe^{-r/l} - e^{-r}$ , where  $fe$  and  $l$  are two constants.

$c$  is a parameter in GOA which is used to balance the exploration and exploitation. The coefficient of  $c$  decreases according to the number of iterations. The value of  $c$  can be computed as follows:

$$c = c^{\max} - u \frac{c^{\max} - c^{\min}}{u^{\max}}, \quad (16)$$

Where,  $c^{\min}$  and  $c^{\max}$  are the minimum and maximum values of  $c$  respectively.  $u^{\max}$  is the maximum number of iterations,  $u$  is the current iteration.

**Algorithm:**

*Weighted FCM with Grasshopper Optimization Algorithm (WFCM-GOA)*

1. Initial class prototype  $\{V_i\}^c$  is selected.
2. All memberships  $b_{ij}$  is updated using the cluster center's weighted average by

$$u_{ik} = \frac{(1 - B(x_k, v_i))^{-\frac{1}{(m-1)}}}{\sum_{j=1}^c (1 - B(x_k, v_j))^{-\frac{1}{(m-1)}}} \quad (17)$$

3. The clusters prototype is obtained as weighted average using

$$v_i = \frac{\sum_{k=1}^n u_{ik}^m B(x_k, v_i) x_k}{\sum_{k=1}^n u_{ik}^m B(x_k, v_i)} \quad (18)$$

4. Initialize the parameters  $c^{\min}, c^{\max}, u, f$  and  $l$
5. Initialize the random population in the search space where  $X^j, \{j=1, 2, 3 \dots N\}$  and initialize the search agent "best"
6. while  $u < u^{\max}$ 
  - a. Evaluate  $c$  using Equation (16)
  - b. For  $i=1: n$  begin
    - i. Update best
    - ii. Normalize the distance between the grasshopper in the range [1,4]
    - iii. Update the position of grasshopper  $X_d^i$  using the equation (15)
    - iv. Check the current grasshopper position if it goes over the boundaries
    - v. End for

- c.  $u = u + 1$ ;
7. End while
8. Return the best solution for updating the weights in WFCM in equation (17) and (18)
9. Continue steps 2-3 until the stopping requirement is satisfied.
10. The criterion for termination is  $|V_{new} - V_{old}| \leq \epsilon$
11. The Euclidean norm is  $\| \cdot \|$ . The cluster centre vector is denoted by  $V$ .  $\epsilon$  is a user-adjustable small number (in this case,  $\epsilon=0.01$ ).
- 12.

The WFCM-GOA algorithm is used in the proposed method to raise the weighted factor for the clustering center without making computation more difficult. Typically, a population aims to evaluate the collective performance of search agents within the current generation. An individual's fitness function value should be lower than the average for a problem to be minimized. As a result, a plan to improve local search should be implemented. Additionally, the population is distributed more randomly. Especially during the later stages of evolution, this property can help population maintain their diversity more effectively.

### 3.4 Feature Extraction

The most crucial method in image processing is image feature extraction. It assumes a significant part in the recognition of malignant growth. To detect cancer, image features are extracted from the image following segmentation. An essential step in the process of predicting cancer and non-cancer in an image is feature extraction. It is the process of identifying and representing particular image features of interest for further processing.

To illustrate the condition and facilitate classifier training, Feature Extraction eliminates specific details from Pap smear images. Recent studies have concentrated on incorporating state-of-the-art feature extraction algorithms for the detection of cervical cancer in Pap smear images. Geometric properties, encompassing asymmetry, diameter, concavity, area, perimeter, and eccentricity, are among the extracted attributes. Additionally, characteristics like shape, size, and texture identification are also considered using GLCM and Haralick features. This approach has previously been applied in the identification of skin lesion images [26].

The calculation of asymmetry is determined by the following equation:

$$A_I = \frac{\Delta A}{A} \times 100 \quad (19)$$

a. Eccentricity is calculated using the below equation:

$$Eccen = \frac{Length_{(Major)}}{Length_{(Minor)}} \quad (20)$$

b. Area of the nucleus can be calculated as:

$$Area_N = \sum_{i=1}^n \sum_{j=1}^m I(i, j) \quad (21)$$

c. Perimeter can be computed using the formula:

$$Perimeter_N = Even_{Count} + \sqrt{2} \times Odd_{Count} \quad (22)$$

Nucleus Diameter can be calculated by the distance between the two points on both the major and minor axis.

### 3.5 Feature Classification using ReLu

The features classification is performed with the Deep Convolutional Network (Deep CNN) with Relu. Here Relu is used as an activation function. In the Deep CNN, organise the network comprises of input layer followed by 2X2 Convolution layers, Pooling layer and 2X2 Convolution layer which is used for the learning step of features. Deep CNN uses the fully connected and softmax layers for its classification stage and is shown in Figure 4.

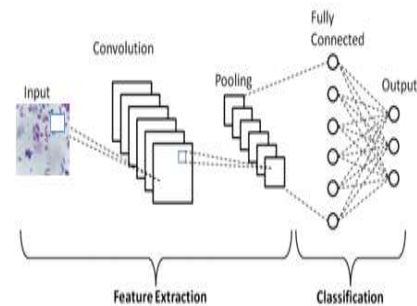


Figure 4: Architecture of Deep CNN with Relu for Detection of Cervical Cancer

#### 3.5.1 Convolutional layer

Each neuron serves as one of the convolutional kernels that make up the convolutional layer. The way a convolutional kernel operates is by slicing the image into tiny



segments, which are called receptive fields. The extraction of features is made easier by breaking up an image into smaller pieces. Kernel multiplies its elements with the corresponding receptive field elements to interact with the images using a particular set of weights. The efficiency of CNN parameters surpasses that of fully connected networks due to the weight-sharing capability of convolutional operations. This enables the extraction of distinct feature sets from an image by sliding a kernel with the same weights across the image.

The Rectified Linear Activation Function, known as ReLU, is a piecewise linear function that directly produces the input if it is positive; otherwise, it returns zero. The utilization of ReLU in a model simplifies the training process and often leads to enhanced performance.

The ReLU function is calculated as

$$R_f = \max(0.0, y) \quad (23)$$

When the value of  $R_f$  reaches to zero, the gradient descent method stops its learning.

### 3.5.2 Pooling Layer:

A Pooling Layer comes next to a Convolution Layer. It works upon each component map independently to make another arrangement of a similar number of pooled include maps. This layer's primary objective is to cut down on computational costs by making the convolved feature map smaller. This is accomplished independently on each feature map by reducing the connections between layers. Here, max pooling has been chosen because it provides the better results than the other pooling methods.

### 3.5.3 Fully connected Layer:

At the network's end, the fully connected layer is typically used for classification. It is a global operation, in contrast to pooling and convolution. Selected features are combined in a non-linear way for the purpose of classifying data. It receives input from the feature extraction phases and performs a global analysis of all previous layers' output.

### 3.5.4 Softmax Layer:

The concluding layer in a Deep Convolutional Neural Network (CNN) is commonly the Softmax layer. Softmax serves as an activation function, transforming numerical values into probabilities. It generates a vector presenting the probabilities of each potential outcome, ensuring that the probabilities of all classes in the vector collectively sum up to one.

## 4. RESULTS & DISCUSSION

### 4.1 Dataset Description

Multicell nucleus of cervical cancer image were collected from SIPaKMeD [28] and Herlev datasets [27] which is utilized in the proposed method. The Herlev dataset, consisting of 917 images, includes cells categorized into classes 1 through 3 representing usual phases, and classes 4 through 7 representing abnormal stages. 4049 cells were cropped from the 966 images that made up the multicell dataset. Here the cells were separated based on benign, normal and abnormal.

### 4.2 Experimental Setup:

Utilising the Matlab 2022b simulation tool, the results were verified. Matlab's Deep Neural Network tool can be used for categorization. The CPU is an Intel (R) Core (TM) i5-3210M with a 2.5GHz CPU and 2.0GB of RAM. Here the proposed Deep CNN with Relu as an activation function is used for feature classification. About 250 sample images are taken into consideration for evaluation. For improved accuracy results, a testing set of 100 sample images and a training set of 150 sample images were used. For validation process, 30% of sample images were used. The trained image size is 250 x 250 pixels which is determined by simulation results of the analysis of MATLAB. Based on the features, the class labels are assigned to values in the hidden nodes, and the relevant values are mapped with the cervical cancer class label. Figure 5 depicts the proposed Deep CNN with Relu classifier in the Pap Smear Image Classification.

### 4.3 Performance Metrics:

The efficiency of the method Deep CNN with Relu as an activation function is evaluated and compared with other classifiers such as RBM, SVM, RF, ELM and RVDLNN. Accuracy, Recall, and Specificity are the

performance criteria used to inspect these methods.

#### 4.3.1 Accuracy:

An estimate of the cervical cancer image's classification accuracy can be calculated by dividing the total number of instances by the number of correctly identified class labels. The accuracy value determines the efficiency of the classification model. The accuracy is measured using the cervical cancer's true positive (TP) and true negative (TN) values. The accuracy is computed by

$$Accuracy = \frac{TP + T}{TP + TN + FP + FN} \quad (24)$$

#### 4.3.2 Recall:

The proportion of positive or correctly categorised values across all instances is referred to as Recall, which is expressed as the rate of TP. It shows the values that were correctly identified after the test, with higher sensitivity indicating lower specificity rates and lower Recall indicating higher specificity rates. The TP value determines the performance of proper identification, and the following evaluation of Recall is provided:

$$Recall = \frac{TP}{TP + FN} \quad (25)$$

#### 4.3.3 Specificity:

The proportion of incorrectly classified values among all cases is referred to as specificity, or the rate of TN, in the medical field. The following is the assessment of specificity, which helps determine whether the classification sample as a whole is correct.

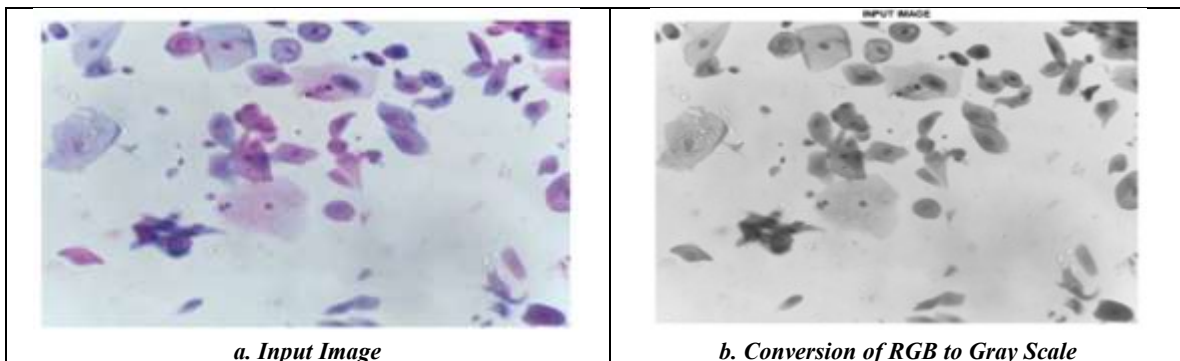
$$Specificity = \frac{TN}{TN + F} \quad (26)$$

#### 4.4 Performance Evaluation:

The performance of the Deep Convolutional Neural Network (CNN) in classifying data is contrasted with the performance of the existing method. Image preprocessing enhances the images, and the optimal segmentation, along with feature selection, is employed to retrieve essential features. The acquired information is then forwarded to the classification phase. A learning rate of 0.001 is utilized in this process. The fully connected layer involves 7 classes, and the batch normalized layer employs 4 channels. These layers encapsulate the extracted features along with their corresponding class labels.

The figure 5.a shows the result of input image that is retrieved from the dataset. Then the image is converted to grayscale image which displays in the figure 5.b. By applying the Dragonfly optimization (DO) in ADF, the test function and result of the preprocessed image shown in figure 5.b and 5.c respectively.

The weighted FCM is used to perform image segmentation on cervical cancer image. In order to optimize the weights, Grasshopper optimization algorithm (GOA) is employed to generate the optimal values of weight in WFCM. This will be very useful for further feature classification by Deep CNN using Relu. From the GOA, optimal score of 0.318 is retrieved. Based on the optimized segmentation results, the network get trained to classify the cervical cancer effectively. The figure 5.e. and 5.f shows the results of GOA convergence of the segmented image and optimized segmented image of cervical cancer image respectively. The figure 5.g. shows the classification of the cervical cancer image.



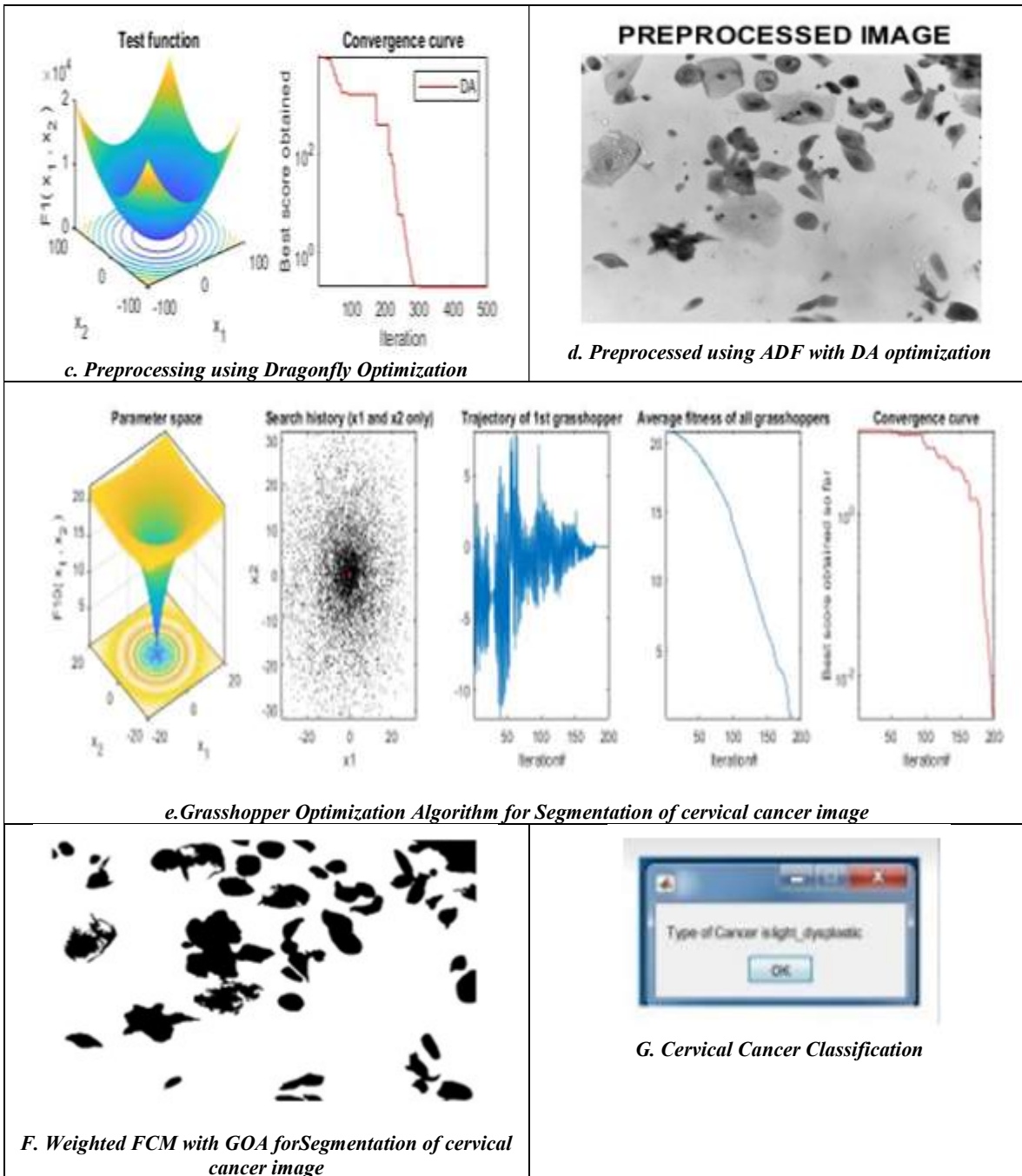


Figure 5: Proposed Deep CNN with Relu based results for detecting Cervical Cancer

#### 4.5 Classification of Cervical Cancer:

With the support of feature selection, the preprocessed and segmented cervical image is

categorised to determine the cervical cancer. Table 1 and Figure 6 show the DCNN classification performance

**Table 1:** Comparison of Cervical cancer classification Performance

Performance Rates	DCNN	RBN	RVDLNN	ELM	SVM	RF
Accuracy (%)	97.8	95.3	88.5	82.65	77.26	78.6
Specificity (%)	91.3	88.6	84.17	81.25	72.19	74.81
Recall (%)	89.8	88.56	76.48	73.44	78.61	71.11

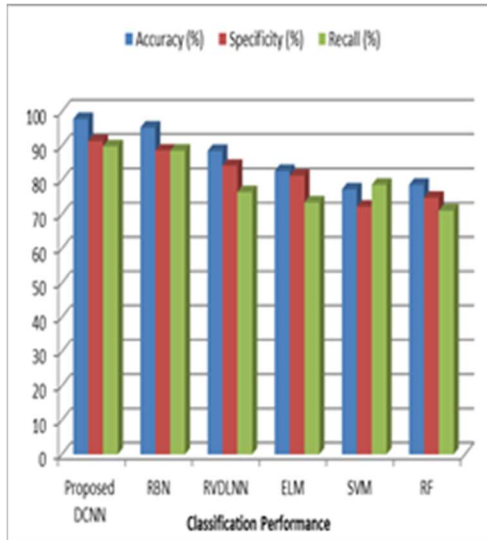


Figure 6: Comparison of Cervical Cancer Performance

The effectiveness of the proposed Deep CNN with Relu and the current method for classifying cervical cancer is shown in Figure 6. Deep CNN outperforms RBN, RVDLNN, ELM, SVM, and RF by 2.5%, 9.3%, 15.15%, 20.6 %, and 19.2%, respectively, in terms of classification accuracy. The classification specificity of Deep CNN outperforms other existing classifiers, including RBN, RVDLNN, ELM, SVM, and RF, by 2.7%, 7.13%, 10.1%, 19.1%, and 16.5%, respectively. Deep CNN is higher than RBN, RVDLNN, ELM, SVM, and RF in terms of classification recall by 1.2%, 13.4%, 16.36%, 11.19%, and 18.69%, respectively. In terms of classification performance, the proposed DCNN performs better than the current method.

The accuracy rate as well as the frequency of error or loss throughout the Deep CNN routine for each iteration is depicted in Figure 7. The pace of exactness increments at cycle 4, and loss diminishes at iteration 2. The reduction of the loss function enhances the performance of Deep

CNN. The classifier's performance is typically assessed using accuracy, while the loss function is employed to enhance and optimize overall performance. As accuracy and iteration increase in Deep CNN, the loss function gets decreases.

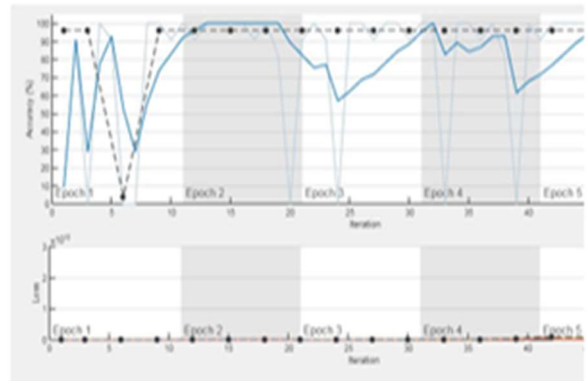


Figure 7: Accuracy and Loss function of Deep CNN with Relu

## 5 CONCLUSION

This article outlines an effective cervical cancer classification technique. In this proposed work mainly focuses on the detection of cervical cancer at earlier stage. The noise in the cervical image is preprocessed using Anisotropic Diffusion filter. The weights of the filter have been optimized through the Dragonfly optimization (DA). So the edges are preserved and also noise gets reduced. Based on the preprocessed image, Weighted FCM with Grasshopper optimization algorithm has been utilized. The needed parts of the segmented image of cervical cancer have been taken out and optimized the features for the phase of feature classification. With the aid of Deep CNN with Relu as an activation function, the features are classified and identify the classification label of cervical cancer effectively. Here, the proposed Deep CNN achieves 97.8% of accuracy than other existing classifiers for cervical cancer classification. Few images are examined through

this classifier and investigation of more images through other novel classifier can be done in the future.

## REFERENCES:

- [1] Tainio K, Athanasiou A, Tikkinen KAO, Aaltonen R, Cárdenas J, Hernández, Glazer-Livson S, Jakobsson M, Joronen K, Kiviharju M, Louvanto K, Oksjoki S, Tähtinen R, Virtanen S, Nieminen P, Kyrgiou M, Kalliala I. Clinical course of untreated cervical intraepithelial neoplasia grade 2 under active surveillance: Systematic Review and Metaanalysis. *BMJ*. 2018 Feb 27; 360:499. DOI: 10.1136/bmj.k499.
- [2] EwertBengtsson, PatrikMalm, "Screening for Cervical Cancer Using Automated Analysis of PAP-Smears", *Computational and Mathematical Methods in Medicine*, vol. 2014, Article ID 842037, 12 pages, 2014. <https://doi.org/10.1155/2014/842037>
- [3] J. Lu, E. Song, A. Ghoneim, and M. Alrashoud, "Machine learning for assisting cervical cancer diagnosis: an ensemble approach," *Future Generation Computer Systems*, vol. 106, pp. 199–205, 2020.
- [4] T. Deepa and A. N. Rao, "A study on denoising of poisson noise in Pap smear microscopic image," *Indian Journal of Science and Technology*, vol. 9, no. 45, 2016.
- [5] J. R. Tang and N. A. M. Isa, "Adaptive image enhancement based on bi-histogram equalization with a clipping limit," *Computers & Electrical Engineering*, vol. 40, no. 8, pp. 86–103, 2014.
- [6] B. Sharma and K. K. Mangat, "Various techniques for classification and segmentation of cervical cell images-a review," *International Journal of Computer Applications*, vol. 147, no. 9, pp. 16–20, 2016.
- [7] R. Saha, M. Bajger, and G. Lee, "Spatial shape constrained fuzzy c-means (fcm) clustering for nucleus segmentation in Pap smear images," in *2016 International conference on digital image computing: techniques and applications (DICTA)*, pp. 1–8, Gold Coast, QLD, Australia, 2016.
- [8] Geetha and Suganya, "A multifaceted tactic for detection of cervical cancer using extreme learning machine with crow search optimization classification", *European Journal of Molecular & Clinical Medicine*, ISSN 2515-8260 Volume 08, Issue 02, 2021, pg.no.934 -944.
- [9] M. A. Devi, S. Ravi, J. Vaishnavi, and S. Punitha, "Classification of cervical cancer using artificial neural networks," *Procedia Computer Science*, vol. 89, pp. 465–472, 2016.
- [10] S. Athinarayanan, M. Srinath, and R. Kavitha, "Computer aided diagnosis for detection and stage identification of cervical cancer by using Pap smear screening test images," *ICTACT Journal on Image & Video Processing*, vol. 6, no. 4, 2016.
- [11] L. Zhang, L. Lu, I. Nogue, R. M. Summers, S. Liu, and J. Yao, "DeepPap: deep convolutional networks for cervical cell classification," *IEEE Journal of Biomedical and Health Informatics*, vol. 21, no. 6, pp. 1633–1643, 2017.
- [12] B. Taha, J. Dias, and N. Werghi, "Classification of cervical-cancer using Pap-smear images: a convolutional neural network approach," in *Annual Conference on Medical Image Understanding and Analysis*, pp. 261–272, Cham, 2017.
- [13] J. Hyeon, H.-J. Choi, K. N. Lee, and B. D. Lee, "Automating papanicolaou test using deep convolutional activation feature," in *2017 18th IEEE International Conference on Mobile Data Management (MDM)*, pp. 382–385, Daejeon, Korea (South), 2017.
- [14] Gautam, Ritu, Prableen Kaur, and Manik Sharma. A comprehensive review on nature inspired computing algorithms for the diagnosis of chronic disorders in human beings. *Progress in Artificial Intelligence*. 2019; 1-24.
- [15] J. Weickert, *Anisotropic diffusion in image processing*. Citeseer, 1998.
- [16] H.Y. Kim, *Gradient Histogram-Based Anisotropic Diffusion*. Personal Communication, 2006.
- [17] G. Sapiro, *Geometric partial differential equations and image analysis*. Cambridge Univ. Pr., 2001
- [18] Mr. P. RAVI , Dr. A. ASHOKKUMAR, "Analysis of Various Image Processing Techniques" *International Journal of Advanced Networking & Applications (IJANA)* Volume: 08, Issue: 05 Pages: 86-

- 89 (2017) Special Issue .Ph.d Research Scholar Department of Computer Science Avinashilingam Deemed University for Women Coimbatore-43
- [19] H.Y. Kim, Gradient Histogram-Based Anisotropic Diffusion. Personal Communication, 2006.
- [20] G. Sapiro, Geometric partial differential equations and image analysis. Cambridge Univ. Pr., 2001
- [21] Reynolds, A.M.; Rhodes, C.J. The Levy flight paradigm: Random search patterns and mechanisms. *Ecology* 2009, 90, 877–887.
- [22] Saremi, S.; Mirjalili, S.; Lewis, A. Grasshopper optimisation algorithm: Theory and application. *Adv. Eng. Softw.* 2017, 105, 30–47
- [23] Nida N., Irtaza A., Javed A., Yousaf M.H., Mahmood M.T., “Melanoma Lesion Detection and Segmentation Using Deep Region Based Convolutional Neural Network and Fuzzy C-Means Clustering”, *Int. J. Med. Inform.* 2019; 124:37–48. Doi: 10.1016/j.ijmedinf.2019.01.005.
- [24] Luo, J.; Chen, H.; Zhang, Q.; Xu, Y.; Huang, H.; Zhao, X.A. An improved grasshopper optimization algorithm with application to financial stress prediction. *Appl. Math. Modell.* 2018, 64, 654–668
- [25] Mafarja, M.; Aljarah, I.; Heidari, A.A.; Hammouri, A.I.; Faris, H.; Al-Zoubi, A.M.; Mirjalili, S. Evolutionary population dynamics and grasshopper optimization approaches for feature selection problems. *Knowl. Based Syst.* 2018, 145, 25–45.
- [26] Zhang, Wenyuan&Guo, Xijuan& Huang, Tianyu& Liu, Jiale& Chen, Jun. (2019). “Kernel-Based Robust Bias-Correction Fuzzy Weighted C-Ordered-Means Clustering Algorithm”, *Symmetry*. 11. 753. 10.3390/sym11060753
- [27] Jantzen, J.; Norup, J.; Dounias, G.; Bjerregaard, B. Pap-smear Benchmark Data for Pattern Classification. *Nature Inspired Smart Information Systems (NiSIS)*.
- [28] Plissiti, M.E.; Dimitrakopoulos, P.; Sfikas, G.; Nikou, C.; Krikoni, O.; Charchanti, A. Sipakmed: A New Dataset for Feature and Image Based Classification of Normal and Pathological Cervical Cells in Pap Smear Images. In Proceedings of the 2018 25th IEEE International Conference on Image Processing (ICIP), Athens, Greece, 7–10 October 2018; pp. 3144–3148.